

# Determination of the Dosimetric Characteristics of BATAN's $^{125}\text{I}$ Source for Brachytherapy: An Experimental Study

K.Y.P. Sandy<sup>1,2</sup>, S.A. Pawiro<sup>1\*</sup> and D.S. Soejoko<sup>1</sup>

<sup>1</sup> Department of Physics, Faculty of Mathematics and Natural Sciences, Universitas Indonesia, Depok 16424, Indonesia

<sup>2</sup> Center for Technology of Radiation Safety and Metrology, National Nuclear Energy Agency, Jl. Lebak Bulus Raya No. 49, Jakarta 12440, Indonesia

## ARTICLE INFO

### Article history:

Received 24 September 2017

Received in revised form 25 March 2018

Accepted 04 April 2018

### Keywords:

Dosimetry

Brachytherapy

Iodine-125

AAPM TG-43

## ABSTRACT

$^{125}\text{I}$  brachytherapy sources with low photon energies have been widely used in treating tumors. According to American Association of Physicists in Medicine Task Group No. 43 (AAPM TG-43) recommendations, dosimetric characteristic of the new brachytherapy sources should be determined before clinical use. In this study, dosimetric characteristic of  $^{125}\text{I}$  manufactured by BATAN have been determined through measurement by using Thermoluminescent Dosemeter (TLD) and gafchromic XR- QA2 film. The radial dose function measurements were performed at distances ranging from 0.5 to 10 cm from the source center. The anisotropy functions were measured at distances of 2, 3, and 5 cm from the source center for angles ranging from 0 to 90 degree in all quadrants. The results indicated that a dose rate constants measured with TLD and film are  $1.05 \pm 8\% \text{ cGy.h}^{-1}.\text{U}^{-1}$  and  $1.01 \pm 8\% \text{ cGy.h}^{-1}.\text{U}^{-1}$ , respectively. The radial dose function decreases along with the increasing distance from source and meets the 5<sup>th</sup> order polynomial equation. The anisotropy function result shows that the anisotropy in dose distribution increases along the source axis. This measurement data are in agreement with the previous study on EGSnrc Monte Carlo result and have a similar pattern with IsoAid and GMS BT-125 commercial  $^{125}\text{I}$  source.

© 2018 Atom Indonesia. All rights reserved

## INTRODUCTION

The dosimetry of source used in brachytherapy has been the subject of considerable researches in recent years. Brachytherapy, using permanently implanted seeds, has become widely accepted for low-risk prostate cancer. It has been proven to be as effective as surgery or external beam radiotherapy [1]. Permanent seed implants have also been used in the treatment of primary and recurrent tumors of the head and neck, lungs, liver, pancreas, rectal, gynecological, and soft tissue [2-4]. The  $^{125}\text{I}$  isotopes are frequently used in low-dose rate (LDR) brachytherapy sources.  $^{125}\text{I}$  source is generated by the neutron activation reaction to the

$^{124}\text{Xe}$  isotope target. This irradiation produces  $^{125}\text{Xe}$  radioisotope that will decay to  $^{125}\text{I}$ . This  $^{125}\text{I}$  decays through electron capture and transforms into  $^{125}\text{Te}$  isotope, producing the maximum photon energy of 35.5 keV by gamma decay. In addition, the transition leads to characteristic x-rays of energy between 27.2 and 31.7 keV (K-shells) as a result of internal conversion [5,6]. Prostate brachytherapy with  $^{125}\text{I}$  sources is a choice for cancer patient treatment with early-stage prostate cancer.  $^{125}\text{I}$  is used because of its low energy emissions, which allow for a rapid decrease in dose with distance, and of its short half-life (59.4 days) [7].

So far, brachytherapy implants using  $^{125}\text{I}$  seeds have not been performed yet in radiotherapy installations in Indonesia, due to many constraints in terms of importation and transportation of  $^{125}\text{I}$  sources from overseas. To meet the market demand

\*Corresponding author.

E-mail address: [supriyanto.p@sci.ui.ac.id](mailto:supriyanto.p@sci.ui.ac.id)

DOI: <https://doi.org/10.17146/aij.2018.719>

in Indonesia, the Center for Technology of Radioisotope and Radiopharmaceutical, National Nuclear Energy Agency of Indonesia (BATAN) has successfully manufactured  $^{125}\text{I}$  seeds that can be used as implantation brachytherapy source. The accuracy of the dosimetry plays an important role in the outcome of brachytherapy. Zelefsky *et al.* [1] found that for patients, whose  $^{125}\text{I}$  dose to 90 % of the prostate ( $D_{90}$ ) was  $\geq 130$  Gy, the 8-year prostate-specific antigen (PSA) relapse-free survival was 93 % compared with 76 % for those with lower  $D_{90}$  dose levels ( $P < 0.001$ ). Stock *et al.* [8] found that the optimal dosimetry of  $^{125}\text{I}$  seed implantation ( $D_{90}$ ) was between 140 and 180 Gy for prostate cancer. The biochemical failure increases when  $D_{90}$  is less than 140 Gy, and the long-term urinary symptoms increase when  $D_{90}$  is more than 180 Gy. A treatment planning system is widely used for seed implantation for preoperative dose calculation, postoperative dose verification, and real-time dose verification [9,10]. One of the most important factors for the dose calculations is the accurate dosimetric parameter of each type of  $^{125}\text{I}$  seed used for implantation [11]. According to the American Association of Physicist in Medicine (AAPM) TG-43 recommendations, dosimetric characteristics of the new brachytherapy sources should be determined before clinical use [12].

The main objective of this project was to determine the dosimetric characteristics of the new iodine brachytherapy source manufactured by BATAN. These dosimetric characteristics were determined using experimental approaches in accordance with the AAPM recommendations in the Task Group 43 protocol [12].

## EXPERIMENTAL METHODS

### BATAN's $^{125}\text{I}$ source

The schematic diagram of  $^{125}\text{I}$  source manufactured by BATAN is illustrated in Fig. 1. The source has a physical length of 4.5 mm and an outer diameter of 0.8 mm. This source was manufactured by placing a 3.0 mm long and 0.5 mm diameter of silver wire covered with  $^{125}\text{I}$  inside a 0.1 mm thick titanium tube. The edges of the cylindrical tube are welded.

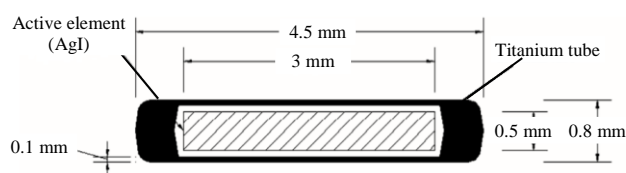


**Fig. 1.** Schematic diagram of  $^{125}\text{I}$  source manufactured by BATAN.

## Dosimetry technique

Dose distributions around the BATAN's  $^{125}\text{I}$  source were measured in an acrylic phantom using TLD-100 LiF thermoluminescence dosimeters and gafchromic XR-QA2 film. For TLD measurements, phantoms were designed based on the phantoms proposed by Meigooni *et al.*, and Hosseini *et al.* [13,14] with dimension of  $30 \times 30 \times 30 \text{ cm}^3$ . The center slabs of acrylic phantom material were customized to accommodate the source and LiF TLD rod with dimensions of  $3 \times 0.8 \text{ mm}$ . Figure 2(a) presents the first phantom that was used for the experimental determination of the  $^{125}\text{I}$  radial dose function values. Holes were drilled in the central phantom slab to accommodate the TLD rod and source. The measurements were performed at distances  $r$  of 0.5, 1, 1.5, 2, 3, 4, 5, 6, 8 and 10 cm relative to center of seed in the spiral configuration. It was to minimize the interference of any TLD with regard to the response by other TLD rod [15,16]. A total of 40 TLDs (four at each radial distance) were used in the experiment due to the configuration of the phantom. The experiment was repeated at least two times to improve the statistical quality of the data. The second phantom (Fig. 2(b)) was used for the measurement of the anisotropy function of the  $^{125}\text{I}$  seed. It has the same geometry and dimensions as the first phantom but differs in the configuration of the source and TLDs hole.

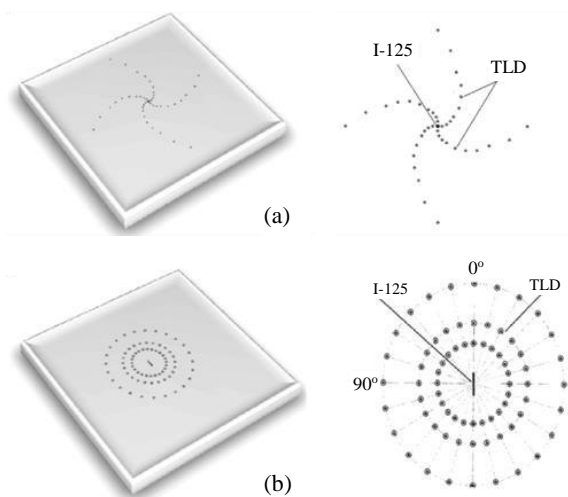


**Fig. 2.** Design of center slab phantom using TLD measurement (a) radial dose function and (b) anisotropy function.

The TLD lies at radial distances  $r$  of 2, 3 and 5 cm relative to center of seed, and polar angles  $\theta$  in the range from  $0^\circ$  to  $90^\circ$  for all quadrants with  $15^\circ$  increments. The measurements were performed at 72 holes containing TLD (four at each radial distance and polar angle). Therefore, since

shadowing was found similar at any polar angle for the same radial distance, the overall effect is cancelled out in the calculation of an anisotropy function. The irradiated TLDs were read using a Harshaw Model 3500 TLD reader and were annealed at 400 °C for 1 hour, followed by 80 °C for 24 hour pre-irradiation annealing.

For gafchromic film measurement, the source was placed inside the phantom as illustrated in Fig. 3. After irradiated, the film was scanned with Film scanner (Microtex 1000XL Plus, Sarasota) and processed with ImageJ software to obtain the value of the dose rate constant, radial dose function, and anisotropy function.

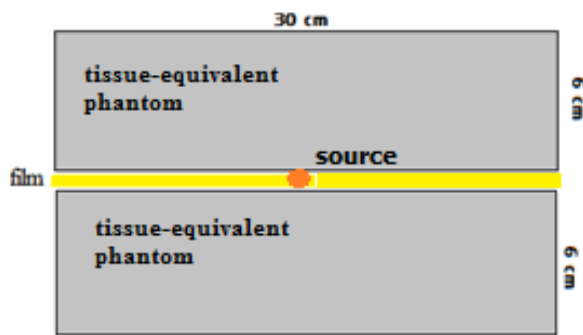


Fig. 3. Measurement scheme for gafchromic XR-QA2 film.

Before the measurement of dose distributions of <sup>125</sup>I source was done, the TLD and gafchromic film had been calibrated before-hand based on those of Meigooni *et al.* and McCabe *et al.* [13,17]. The calibration was done by exposing the TLD and film to various doses using Secondary Standards Dosimetry Laboratory (SSDL) Jakarta standard X-ray machine (Y.TU 320-D03 YXLON, Hamburg) with radiation energy of 28 keV and quality of 0.82 mmAl HVL. This calibration condition was suited to energy of <sup>125</sup>I.

Air kerma strength of <sup>125</sup>I also has to be determined before the measurement of dose distribution [18,19] using Bohm extrapolation chamber. Extrapolation chamber, which had been connected with Unidos electrometer, was placed at a distance of 10 cm from the source <sup>125</sup>I. Measurements were made with 1 mm to 10 mm electrode gap and a predetermined voltage range ± (30-70) V / mm with a maximum voltage of 500 V. The measurements were repeated seven times for each electrode gap both for positive and negative polarity.

The characteristics of the BATAN <sup>125</sup>I source were determined experimentally based on the AAPM TG-43 recommendations. Following this protocol, the distributions of the absorbed dose rate around a sealed brachytherapy source can be determined by using Equation 1:

$$\dot{D}(r, \theta) = S_k \cdot \Lambda \cdot \frac{G(r, \theta)}{G(r_o, \theta_o)} \cdot g(r) \cdot F(r, \theta) \quad (1)$$

where  $S_k$  is the air kerma strength,  $\Lambda$  is the dose rate constant,  $G(r, \theta)$  is the geometry function,  $g(r)$  is the radial dose function, and  $F(r, \theta)$  is the anisotropy function. The dose rate constant is defined as:

$$\Lambda = \frac{D(r_o, \theta_o)}{S_k} = \frac{D(1 \text{ cm}, \frac{\pi}{2})}{S_k} \quad (2)$$

The radial dose function,  $g(r)$  describes the attenuation in tissue of the photons emitted from the brachytherapy source. The radial dose function is defined as:

$$g(r) = \frac{D(r, \frac{\pi}{2})}{D(1, \frac{\pi}{2})} \frac{G_L(1, \frac{\pi}{2})}{G_L(r, \frac{\pi}{2})} \quad (3)$$

where  $D(r, \pi/2)$  and  $D(1, \pi/2)$  are the dose rates measured at distances of  $r$  and 1 cm, respectively, along the transverse axis of the source.  $G_L(r, \theta)$  is known as the geometry function that takes into account the effect of the distribution of radioactive material inside the capsule on the dose distribution [20].  $G_L(r, \theta)$  is a function of  $r$  which is equal to distance from the source center, polar angle  $\theta$ , and  $L$  the effective length of source. The geometry function is defined by the AAPM TG-43 as:

$$G(r, \theta) = \begin{cases} r^{-2}, & \text{point source approximation} \\ (r^2 - L^2/4)^{-2}, & \text{line source approximation } \theta = 0 \\ \frac{\beta}{Lr \sin \theta}, & \text{line source approximation } \theta \neq 0 \end{cases} \quad (4)$$

The anisotropy function was calculated following the TG-43 recommendation as:

$$F(r, \theta) = \frac{D(r, \theta)}{D(r, \frac{\pi}{2})} \frac{G_L(r, \frac{\pi}{2})}{G_L(r, \theta)} \quad (5)$$

## RESULTS AND DISCUSSION

The dose rate constant of BATAN's <sup>125</sup>I source was measured by using LiF TLD and gafchromic XR-QA2 film in an acrylic phantom. The measured dose rate constant in acrylic was then multiplied by 1.05 to obtain the dose rate constant of the <sup>125</sup>I source in water [21]. The TLD measured dose rate constant of the BATAN <sup>125</sup>I source in acrylic and water was found to be  $1.00 \pm 8 \%$  cGy.h<sup>-1</sup>.U<sup>-1</sup> and  $1.05 \pm 8 \%$  cGy.h<sup>-1</sup>.U<sup>-1</sup>, respectively. Meanwhile the gafchromic measured dose rate in acrylic and water was found to be  $0.96 \pm 8 \%$  cGy.h<sup>-1</sup>.

$1.U^{-1}$  and  $1.01 \pm 8 \%$   $cGy.h^{-1}.U^{-1}$ , respectively. Furthermore, the dose rate constant determined in this study will be compared with Monte Carlo simulation results in the previous study by Budiantari [22] as well as other commercially available sources, which are illustrated in Table 1. The difference of the dose rate constants varied with different coating thicknesses, coating mass densities, photon interaction cross-section libraries, and photon emission spectrum types [23]. Aryal P. et al. [24] found that varying  $^{125}I$  coating thickness, coating mass density, photon cross-section library, and photon emission spectrum for the model IA125I A  $^{125}I$  seed changed the dose rate constant by up to 0.9 %, about 1 %, about 3 %, and 3 %, respectively, in comparison to the proposed standard value of  $0.922 cGy.h^{-1}.U^{-1}$ . Table 2 shows the propagation of error during these data analysis.

**Table 1.** Dose rate constants determined in this work compared with previous studies

| Source $^{125}I$    | Method            | Medium      | $\Lambda$<br>cGy.h <sup>-1</sup> .U <sup>-1</sup> |
|---------------------|-------------------|-------------|---|
| BATAN $^{125}I$     | TLD Measurement   | Acrylic     | 1.00  |
|                     | Measured*         | Water       | 1.05  |
| BATAN $^{125}I$     | Film Measurement  | Acrylic     | 0.96  |
|                     | Measured*         | Water       | 1.01  |
| BATAN $^{125}I$     | MonteCarlo EGSnrc | Water       | 1.01  |
| IA $^{125}I$ IsoAid | TLD Measurement   | Solid Water | 0.99  |
|                     | Measured*         | Water       | 1.03  |
| GMS BT-125-1        | MonteCarlo MCNP5  | Water       | 0.98  |

\*Obtained by multiplying the measured data in Solid Water by 1.05 [22]

**Table 2.** Propagation of error in the experimental determination of the dose rate distribution

| Component of uncertainty                      | Type A | Type B |
|---|--------|--------|
|   | ( % )  | ( % )  |
| Repetitive measurements                       | 4.0    |        |
| Detector dose calibration                     |        | 3.0    |
| Correction for energy dependence of dosimeter |        | 5.0    |
| Seed and detector positioning                 |        | 1.0    |
| Total uncertainty ( 1 -sigma )                |        | 7.1    |
| SSDL air kerma measurement uncertainty        |        | 3.5    |
| Total combined uncertainty                    |        | 8      |

The radial dose function of BATAN's  $^{125}I$  brachytherapy source was extracted from the absorbed dose measured in acrylic phantom material from 0.5 to 10 cm with 0.5 to 2 cm increment from the source center. An active length of 3.0 mm was used for this source during the calculation of the geometric functions. The data at each radial distance were obtained from the average of at least 8 TLD with a standard deviation of about  $\pm 5 \%$  can be seen in Table 3. It demonstrates that the radial dose functions of BATAN's  $^{125}I$  measured with TLD are

in good agreement with the radial dose functions measured with film gafchromic. Furthermore, the comparison of the radial dose function  $g(r)$  in the acrylic medium with Monte Carlo simulation results as well as other commercially available sources is illustrated in Fig. 4. As derived from Fig. 4, the  $g(r)$  values in this work have a similar pattern with the published Monte Carlo simulation results and also with  $g(r)$  for IA  $^{125}I$  IsoAid and GMS BT-125-1  $^{125}I$  brachytherapy sources. The pattern shows that the  $g(r)$  values will decrease along with the increasing distance from the source as the result of the attenuation effect of medium [25].

**Table 3.** Radial dose function of BATAN  $^{125}I$  source measurement using TLD and gafchromic film

| $r$ ( cm ) | $g(r)$ |       |
|------------|--------|-------|
|            | TLD    | Film  |
| 0.5        | 1.059  | 1.172 |
| 1.0        | 1.000  | 1.000 |
| 1.5        | 0.834  | 0.887 |
| 2.0        | 0.806  | 0.763 |
| 3.0        | 0.636  | 0.655 |
| 4.0        | 0.525  | 0.561 |
| 5.0        | 0.503  | 0.452 |
| 6.0        | 0.316  | 0.341 |
| 7.0        | -      | 0.254 |
| 8.0        | 0.167  | 0.207 |
| 9.0        | -      | 0.174 |
| 10.0       | 0.077  | 0.122 |

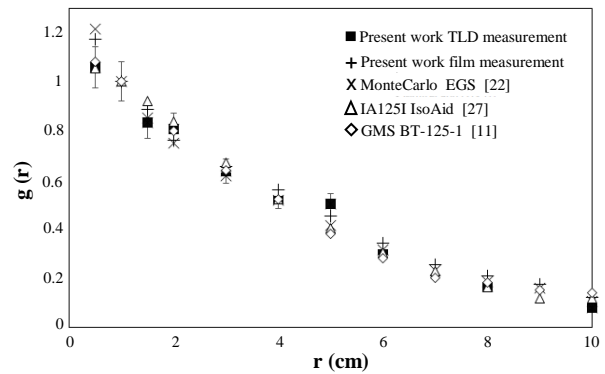


**Fig. 4.** Radial dose function  $g(r)$  determined in the present work compared with previous studies.

For clinical applications,  $g(r)$  was fitted to a fifth-order polynomial function as follows [26]:

$$g(r) = a_0 + a_1r^1 + a_2r^2 + a_3r^3 + a_4r^4 + a_5r^5 \quad (6)$$

where the coefficient of  $a_0$  to  $a_5$  values in this work are presented in Table 4. The tabulated obtained data or coefficients of these fifth order polynomials can be entered as the input of treatment planning systems for dose estimation at each distance from the source.

**Table 4.** Coefficient for radial dose function fit to fifth order polynomial

| Measurement | $a_0$<br>( $\times 10^0$ ) | $a_1$<br>( $\times 10^{-1}$ ) | $a_2$<br>( $\times 10^{-2}$ ) | $a_3$<br>( $\times 10^{-3}$ ) | $a_4$<br>( $\times 10^{-4}$ ) | $a_5$<br>( $\times 10^{-5}$ ) |
|-------------|----------------------------|-------------------------------|-------------------------------|-------------------------------|-------------------------------|-------------------------------|
| TLD         | 1,1952                     | -2,5963                       | 2,8224                        | 4,8395                        | -5,0504                       | 3,2235                        |
| Film        | 1,4335                     | -6,1094                       | 2,1217                        | -4,2202                       | 3,9522                        | -1,3738                       |

The anisotropy function,  $F(r,\theta)$  of  $^{125}\text{I}$  source was measured at  $15^\circ$  angle increments relative to the source axis at distances of 2, 3, and 5 cm from the source center in the acrylic medium. The results are illustrated in Fig. 5 and Fig. 6. They show that the values of  $F(r,\theta)$  are unified at the transverse axis of the source ( $\theta = 90^\circ$ ) and decrease as  $\theta$  approaches  $0^\circ$ . This decrease in  $F(r,\theta)$  was due to the increase in the thickness of source encapsulations towards the longitudinal axis of the source [25]. To further analyze the anisotropy function data, a comparison  $F(r,\theta)$  value at a radial distance of 3 cm was made between measurements using the TLD and gafchromic film as shown in Fig. 6. Figure 6 also shows the comparison between  $F(r,\theta)$  for this work and Monte Carlo previous result as well as other commercial source. Figure 6 illustrates that the value of  $F(r,\theta)$  measurements using the TLD and gafchromic film has a significant difference in the angle less than  $30^\circ$ , while for angel more than  $30^\circ$  the differences are not significant. Compared to previous study,  $F(r,\theta)$  in this work has a similar pattern with the published Monte Carlo simulation and with  $F(r,\theta)$  for IA $^{125}\text{I}$  IsoAid [27] commercial  $^{125}\text{I}$  source for brachytherapy. However there are still different values of  $F(r,\theta)$  particularly for the angle less than  $20^\circ$ . It may be due to the accurate simulation of the shape of the end weld, which is relevant for two-dimensional anisotropy function values at small angles. The differences between the measured and the Monte Carlo simulated  $F(r,\theta)$  are seen to increase with the decreasing polar angle. These differences can be mainly attributed to the accuracy of the Seed or TLD positioning, the simulation of the end weld thickness, seed design, and distribution of radioactivity within the seed.

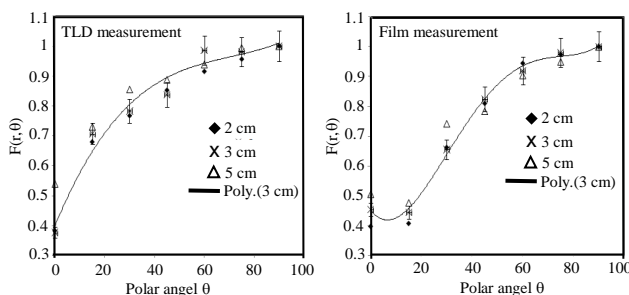


**Fig. 5.** Anisotropy function  $F(r,\theta)$  determined in present work.

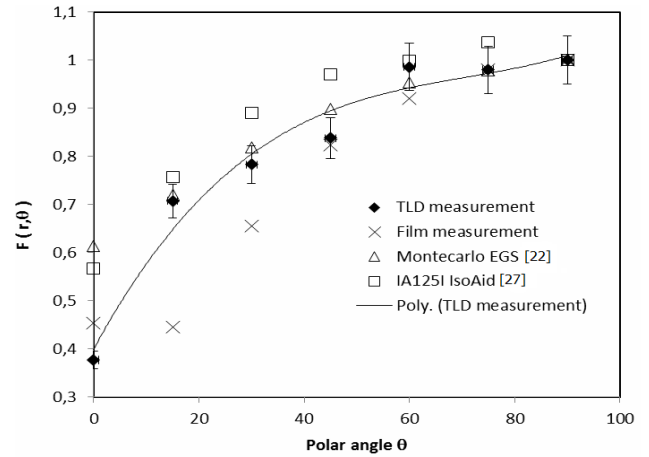


**Fig. 6.** Anisotropy function  $F(r,\theta)$  determined in present work at 3 cm radial distance compare with previous studies.

**CONCLUSION**

This work is the first study to determine the dosimetric characteristic of BATAN's  $^{125}\text{I}$  seed by using experimental measurements. The measured TLD and gafchromic dose rate constant for BATAN's  $^{125}\text{I}$  source shows good agreement with the Monte Carlo simulation result. The dose rate constant of the BATAN's  $^{125}\text{I}$  source is similar to that of the IA $^{125}\text{I}$  IsoAid seed and the GMS BT-125-1 seed. The radial dose function for BATAN's  $^{125}\text{I}$  source measurement in acrylic medium using TLD and gafchromic detector has a similar pattern with the Monte Carlo simulation result and with IA $^{125}\text{I}$  IsoAid and GMS BT-125-1 commercial  $^{125}\text{I}$  source. The pattern shows that the  $g(r)$  values decrease along with the increased distance from the source and meet the fifth order polynomial equation. The anisotropy function result also has similar pattern with the Monte Carlo simulation result and with IA $^{125}\text{I}$  IsoAid. The anisotropy in dose distribution around the source increases along the source axis.

**ACKNOWLEDGMENT**

This project was supported by the research grant from the University of Indonesia with contract number of 540/UN2.R12/HKP.05.00/ 2015, Annual Research Project of the Center for Technology of Radiation Safety and Metrology, and scholarship from the Center for Education and Training, National Nuclear Energy Agency of Indonesia.

**REFERENCES**

1. M.J. Zelefsky, D.A. Kuban, L.B Levy *et al.*, Int. J. Radiat. Oncol. Biol. Phys. **67** (2007) 327.

2. L. Zhu, Y. Jiang, J. Wang *et al.*, *World J. Surg. Oncol.* **11** (2013) 60.
3. Z. Xiang, G. Li, Z. Liu *et al.*, *Med. (Baltimore)* **94** (2015) 2249.
4. C. Ren, R. Shi, L. Min *et al.*, *Clin. Oncol. (R. Coll. Radiol.)* **26** (2014) 230.
5. Maiyesni, Mujinah, Witarti *et al.*, *Journal of Valence* **3** (2013) 65. ( in Indonesian)
6. J. Pouliot and L. Beaulieu, *Leibel and Phillips Textbook of Radiation Oncology*, 3<sup>rd</sup> ed., Elsevier Inc. Saunders, Netherlands (2010) 224.
7. R. Deshmukh, A.N. Singh, M. Martinez *et al.*, *Side Effect of Drugs Annual.* **38** (2016) 443.
8. R.G. Stock, N.N. Stone, M. Dahlal *et al.*, *Brachytherapy* **1** (2002) 83.
9. R.S. Davies, T. Perrett, J. Powell *et al.*, *Med. Dosim.* **41** (2016) 290.
10. M.J. Zelefsky, G.N. Cohen, A.S. Taggar *et al.*, *Pract. Radiat. Oncol.* **7** (2017) 319.
11. N. Zhao, R. Yang, L. Ren *et al.*, *J. Appl. Clin. Med. Phys.* **18** (2017) 49.
12. M.J. Rivard, B. Coursey, L. DeWerd *et al.*, *Med. Phys.* **31** (2004) 633.
13. A.S. Meigooni, D.M. Gearheart and K. Sowards, *Med. Phys.* **27** (2000) 2168
14. S.H. Hosseini, M. Sadeghi and V. Ataeinia, *Med. Phys.* **36** (2009) 3080
15. M. Sadeghi, S.H. Hosseini and G. Raisali, *Appl. Radiat. Isot.* **66** (2008) 1431.
16. H. Safigholi, D. Sardari, J.S. Karimi *et al.*, *J. Appl. Clin. Med. Phys.* **14** (2013) 4226.
17. B.P. McCabe, M. Speidel, T.L. Pike *et al.*, *Med. Phys.* **38** (2011) 1919.
18. H-J. Selbach, H-M Kramer and W.S. Culberson, *Metrologia* **45** (2008) 422.
19. M. Golshan, I. Spadinger and N. Chang, *Med. Phys.* **43** (2016) 3008
20. P. Saidi, M. Sadeghi, A. Shirazi *et al.*, *Appl. Phys. Med.* **28** (2012) 13.
21. J.F. Williamson, *Med. Phys.* **18** (1991) 776.
22. C.T. Budiantari, Determination of the Dosimetric Parameter of the <sup>125</sup>I Brachytherapy Source Manufacturing by BATAN with Monte Carlo Simulation and Experimental Method, Thesis, Universitas Indonesia (2014). (in Indonesian)
23. L.A. DeWerd, G.S. Ibbott, A.S. Meigooni *et al.*, *Med. Phys.* **38** (2011) 782.
24. P. Aryal, J.A. Molloy and M.J. Rivard, *Med. Phys.* **41** (2014) 021702.
25. M. Zehtabian, R Faghihi and S. Sina, *Iran J. Radiat. Res.* **7** (2010) 217.
26. P. Saidi, M. Sadeghi, S.H. Hosseini *et al.*, *J. Appl. Clin. Med. Phys.* **12** (2011) 286.
27. A.S. Meigooni, J.L. Hayes, H. Zhang *et al.*, *Med. Phys.* **29** (2002) 2152.